

# Hydrothermal Stability and Performance of Silica-Zirconia Membranes for Hydrogen Separation in Hydrothermal Conditions

KAZUHIRO YOSHIDA<sup>1</sup>, YOSHIO HIRANO<sup>1</sup>,  
HIRONORI FUJII<sup>2</sup>, TOSHINORI TSURU<sup>3</sup>  
AND MASASHI ASAEDA<sup>3</sup>

<sup>1</sup>Technical Research Center, The Chugoku Electric Power Co., Inc.,  
Higashi-Hiroshima 739-0046, Japan

<sup>2</sup>The Chuden Kankyo Technos Co., Ltd.,  
Higashi-Hiroshima 739-0046, Japan

<sup>3</sup>Department of Chemical Engineering, Hiroshima University,  
Higashi-Hiroshima 739-8527, Japan

**Keywords:** Inorganic Membranes, Sol-Gel Method, Hydrogen Separation, Gas Separation, Silica

Three types of silica-zirconia membranes of different zirconia content were prepared by the sol-gel method to test their stability and H<sub>2</sub> separation performance in hydrothermal conditions. Some silica-zirconia membranes were prepared by “steam-firing” in which firing was carried out in steamed air in order to increase the hydrothermal stability, and then tested in hydrothermal conditions. The activation energy of H<sub>2</sub> and He permeation increased with increasing zirconia content, suggesting that the networks of silica-zirconia matrix were densified with increasing zirconia content. In the hydrothermal conditions, the activation energy of H<sub>2</sub> and He permeation also increased, indicating clearly that silica-zirconia membranes were also densified by water vapor at high temperature. The pores for N<sub>2</sub>, CO<sub>2</sub> and CH<sub>4</sub> permeation decreased with the increasing zirconia content and vanished in the hydrothermal conditions, leaving some pinholes. Some silica-zirconia membranes were prepared by firing in steamed air in order to increase the hydrothermal stability. This method appeared to be effective to increase hydrothermal stability of the silica-zirconia membrane.

## Introduction

In recent years, CO<sub>2</sub> emissions from fossil fuels combustion are considered one of the major causes of global warming. In compliance with the conclusion of the Kyoto Protocol in COP3 (The 3rd Session of the Conference of the Parties to the United Nations Framework Convention on Climate Change in 1997), Japan is obliged to reduce her overall emission of the greenhouse gases by at least 6 per cent below the 1990 level in the commitment period 2008 to 2012. The electric power companies have been conducting activities to form energy supply structures with less CO<sub>2</sub> exhaust such as promoting nuclear power generation and introducing high-efficiency power generation systems. Until now, we have depended on a lot of electricity from thermal power stations, consuming coal, petroleum and natural gas. This trend would be continued for a while, since the new energy systems such as solar power generation systems, wind power generation systems and fuel cell systems will take many more years to be put in practice in a large scale. In addition,

the demand for electricity will continue to increase in the near future, causing more CO<sub>2</sub> emissions. For the stable energy supply, we will be required to reduce CO<sub>2</sub> emissions from thermal power stations by developing new systems for CO<sub>2</sub> reduction.

Many researches have been reported on the CO<sub>2</sub> reduction from the boiler flue gas by chemical absorption, physical adsorption or membrane separation (Mimura and Stumi, 1998; Mimura *et al.*, 1998, 2000; Matsumiya *et al.*, 1999). In case of CO<sub>2</sub> recovery from the conventional fossil fuel power generation systems, however, a higher power cost would be inevitable because of the cost increase on the extra equipment and the decline of thermal efficiency. On the other hand, as one of the most efficient strategies of the reduction in CO<sub>2</sub> emissions from thermal power stations has been proposed “the LNG reforming combined cycle power generation system with the H<sub>2</sub>-separation membrane” (Morinaga *et al.*, 1992; Takahashi *et al.*, 1999). In this system, natural gas is reformed into H<sub>2</sub>, CO, etc. H<sub>2</sub> is removed from the reforming reactor simultaneously by using H<sub>2</sub>-separation membranes. The residual gases including CH<sub>4</sub> and CO are burned at an after-burner with pure O<sub>2</sub> to give exhaust gas of a high CO<sub>2</sub> concentration, which can be easily recovered. H<sub>2</sub> removed from the reactor is fed to a gas turbine generation system.

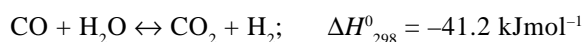
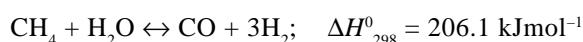
Received on September 6, 2000. Correspondence concerning this article should be addressed to K. Yoshida (E-mail address: 352357@pnet.energia.co.jp).

**Table 1** Starting composition of silica-zirconia colloidal sols and average diameters of colloidal particles measured by laser light scattering system

Composition [ZrO <sub>2</sub> mol%]		TEOS [g]	ZTBO [g]	H <sub>2</sub> O [g]	HCl (35%) [g]	C <sub>2</sub> H <sub>5</sub> OH [g]	Colloidal diameter* [nm]
10 (S9-Z1)	sol-A	4.15	0.85	1.99	0.59	207	49.1
	sol-B	3.32	0.68	1.60	0.59	165	35.3
	sol-C	1.66	0.34	0.80	0.59	82.7	10.2
30 (S7-Z3)	sol-A	5.59	4.41	3.45	0.59	179	33.7
	sol-B	4.19	3.31	2.59	0.59	134	19.5
	sol-C	1.83	1.44	1.13	0.59	117	7.6
50 (S5-Z5)	sol-A	5.10	9.40	4.41	0.59	229	47.9
	sol-B	4.41	7.45	3.50	0.59	181	22.4
	sol-C	1.41	2.59	1.22	0.59	94.6	8.3

\*after boiling the polymer solution for about 30 hours adding water and acid to the solution

Methane steam reforming involves the following main reactions:



High temperature and low-pressure are thermodynamically favorable conditions for the reactions, because the overall reforming reaction is endothermic and it gives the increase in mole number of the participating gases. If H<sub>2</sub> is selectively removed from the reaction system, the thermodynamic equilibrium position of these reactions can be shifted to the product side, giving a higher conversion of CH<sub>4</sub> to H<sub>2</sub> and CO<sub>2</sub> even at lower temperatures (Kikuchi, 1996). The key technology in the system mentioned above is the development of thermally stable H<sub>2</sub>-separation membranes in LNG reformed fuel gas processes. Inorganic separation membranes could be such membranes because of their provable high stability at high temperature.

Inorganic membranes have attracted increasing attention in the field of membrane science and technology because of their thermal and chemical stability. Many researchers have studied on the fabrication procedures of ceramic membranes by the chemical vapor deposition (CVD) and sol-gel methods. Amorphous silica (SiO<sub>2</sub>) membranes have been shown to have a high H<sub>2</sub>-selective permeance and high stability in dry gases at high temperature (Gavalas and Megris, 1989; Kitao *et al.*, 1990). In hydrothermal conditions, however, the H<sub>2</sub> permeance of the CVD derived SiO<sub>2</sub> membrane decreased drastically probably because of densification of silica matrix by water vapor at high temperature (Tsapatsis and Gavalas, 1994; Kim and Gavalas, 1995). Since the gas mixtures from LNG reforming processes contain high concentration of water vapor, the membranes are essentially required of the high stability in hydrothermal conditions.

Composite membranes of silica with the inorganic oxide such as titania (TiO<sub>2</sub>) and zirconia (ZrO<sub>2</sub>) are reported as better alternatives to silica membranes. These materials may combine the processing flexibility of silica together with better stability against thermally and chemically aggressive environments. Nogami and Moriya (1977) reported that the addition of TiO<sub>2</sub> or ZrO<sub>2</sub> to SiO<sub>2</sub> was effective for the improvement of alkali resistance. The silica-zirconia (SiO<sub>2</sub>-ZrO<sub>2</sub>) composite H<sub>2</sub>-separation membranes were successfully prepared by the sol-gel method (Tsuru *et al.*, 1996). Efforts to improve the hydrothermal stability of the SiO<sub>2</sub> membrane by adding alumina (Al<sub>2</sub>O<sub>3</sub>) are also in progress (Ha *et al.*, 1998). For an application to the iodine-sulfur process, the CVD derived silica membranes were examined in H<sub>2</sub>-H<sub>2</sub>O-HI gaseous mixtures (Hwang *et al.*, 2000). The CVD derived SiC-based membranes were also examined in H<sub>2</sub>-H<sub>2</sub>O-HBr system (Sea *et al.*, 1998). The hydrophobic silica membranes were also prepared by incorporation of methyl groups in the silica microstructure (de Vos *et al.*, 1999). On the other hand, SiO<sub>2</sub> membranes were reported to become quite sable against steam at high temperature by keeping coated membranes in humid air for a few days and firing them in steam (Asaeda and Kashimoto, 1998).

In this work, three types of SiO<sub>2</sub>-ZrO<sub>2</sub> membranes with different ZrO<sub>2</sub> contents were prepared by the sol-gel methods. The SiO<sub>2</sub>-ZrO<sub>2</sub> membranes were fired in air and in steamed air to test their stability and H<sub>2</sub> separation performance in hydrothermal conditions. The effects of ZrO<sub>2</sub> contents and steam treatments on H<sub>2</sub> permeance are discussed in details.

## 1. Experimental

### 1.1 Preparation of colloidal sols

SiO<sub>2</sub>-ZrO<sub>2</sub> composite colloidal sols of molar ratios 9/1, 7/3 and 5/5 were prepared by hydrolysis and

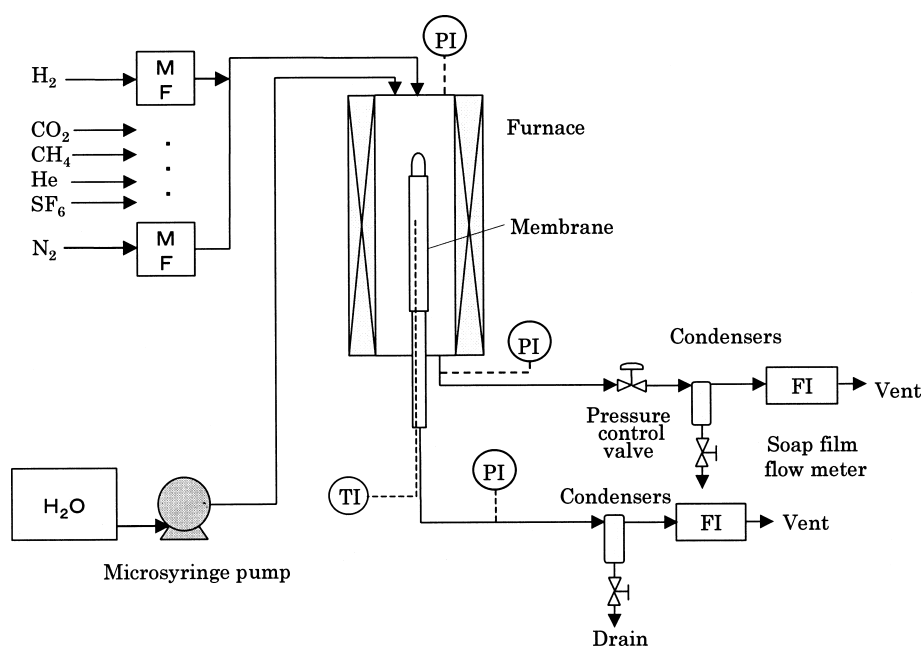


Fig. 1 Schematic diagram of the experimental set-up

condensation reactions of tetraethoxysilane (TEOS) and zirconium-tetra-butoxide (ZTBO). TEOS was partially pre-hydrolyzed in ethanol and then added ZTBO for 30 minutes of hydrolysis and condensation reactions to obtain  $\text{SiO}_2\text{-ZrO}_2$  polymer sol at  $4^\circ\text{C}$ . After adding a large amount of water and hydrochloric acid in order to control the concentration and pH, the solution was boiled for 30 hours to obtain a colloidal sol. The starting compositions of the sols prepared are shown in **Table 1**. The average colloid diameters of the sols were measured by a laser light scattering system (Zetasizer2000HS, Malvern Instruments).

### 1.2 Preparation of $\text{SiO}_2\text{-ZrO}_2$ membranes

Three types of  $\text{SiO}_2\text{-ZrO}_2$  membranes of molar ratios 9/1 (S9-Z1), 7/3 (S7-Z3) and 5/5 (S5-Z5) were prepared by coating the sol on cylindrical  $\alpha$ -alumina porous tubes (average pore diameter:  $1\ \mu\text{m}$ , outer diameter: 1 cm, length: 9 cm). First of all,  $\alpha$ -alumina particles of average diameters 1.84, 0.64 and  $0.2\ \mu\text{m}$ , were coated on the outer surface of the tubes with sol-A as a binder to make the surface sufficiently flat and to reduce the pore diameter. The hot coating method (Asaeda *et al.*, 1992) was applied. The substrate, which was heated approximately up to  $190^\circ\text{C}$ , was coated with the diluted sol solution, then it was fired at  $570^\circ\text{C}$  for 15 minutes in a temperature-controlled electric furnace. These procedures were repeated several times with the sols of larger particle diameter to smaller one. Some of the  $\text{SiO}_2\text{-ZrO}_2$  membranes of molar ratio 9/1 were also prepared by firing in steamed air (50 vol% of steam) at  $570^\circ\text{C}$ .

### 1.3 Measurements of gas permeance

In the first step, permeances of pure He,  $\text{H}_2$ ,  $\text{N}_2$ ,  $\text{CO}_2$ ,  $\text{CH}_4$  and  $\text{SF}_6$  were measured in the temperature

Table 2 Experimental conditions (feed) of hydrothermal stability tests

	Partial pressure [kPa]			Total pressure [kPa]	Temperature [K]
	$\text{H}_2\text{O}$	$\text{H}_2$	$\text{N}_2$		
Test I	40	130	130	300	773
Test II	100	100	100	300	773
Test III	200	200	200	600	773

range of  $200\text{--}500^\circ\text{C}$  by using an apparatus schematically shown in **Fig. 1**. The gas flow rate on the feed side was controlled by mass flow controllers and a pressure control valve to maintain the pressure difference across the membrane at 0.1 MPa, while the permeate side was kept at the atmospheric pressure. The permeation rate was measured by a soap film flow meter (SF-1, STEC).

In the second step, the  $\text{SiO}_2\text{-ZrO}_2$  membranes were hydrothermally treated at  $500^\circ\text{C}$  in a gas mixture ( $\text{H}_2$ ,  $\text{N}_2$  and  $\text{H}_2\text{O}$ ). The composition of the gas mixture was controlled by mass flow controllers and by a micro-syringe pump. The experimental conditions of hydrothermal stability tests are shown in **Table 2**. The pressure on the permeate side was maintained at the atmospheric pressure in these tests. After specified time intervals of hydrothermal treatments, the water feed was stopped and the permeation cell was dried completely before measurements of pure  $\text{H}_2$  and  $\text{N}_2$  permeances. After 10 hours of each hydrothermal stability test, the temperature dependency of the permeances of the pure gases were measured in the temperature range  $200\text{--}500^\circ\text{C}$ .

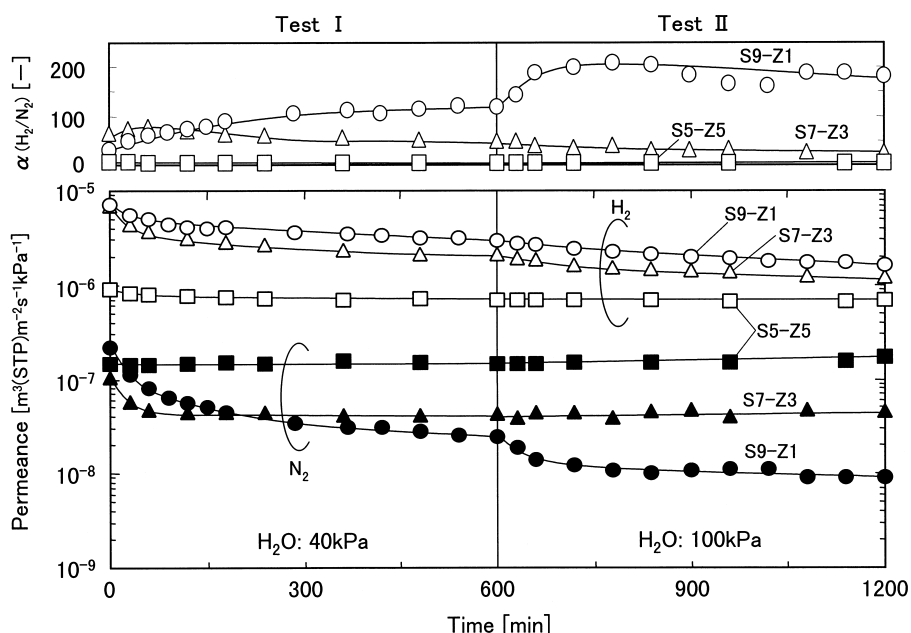


Fig. 2 Permeances of pure  $H_2$  and  $N_2$  and  $\alpha(H_2/N_2)$  at  $500^\circ C$  as a function of hydrothermal time. Partial pressure of  $H_2O$ : 40 kPa (0–600 min), 100 kPa (600–1200 min)

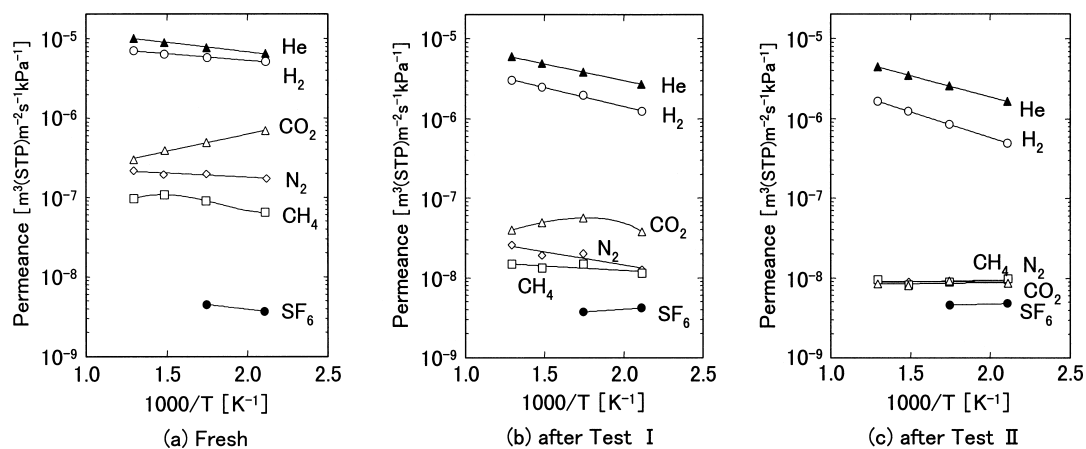


Fig. 3 Arrhenius plots of permeances through the S9-Z1 membrane before and after hydrothermal stability tests

## 2. Results and Discussion

### 2.1 Hydrothermal stability of $SiO_2-ZrO_2$ membranes

Figure 2 shows the observed permeance changes of pure  $H_2$  and  $N_2$  during the hydrothermal tests at  $500^\circ C$ . In the test I (partial pressure of water vapor; 40 kPa), the permeances of  $H_2$  and  $N_2$  through S9-Z1 and S7-Z3 membranes decreased drastically during the first 60 minutes, and slightly from 60 to 600 minutes, and approached to constant values. Under a higher partial pressure of water vapor (100 kPa) in test II, the  $H_2$  permeances of S9-Z1 and S7-Z3 membranes decreased gradually, while  $N_2$  permeance of S9-Z1 membrane decreased drastically, but that of S7-Z3 membrane showed little change. After test II, the S9-Z1

membrane showed a permeability ratio  $\alpha(H_2/N_2)$  of 190 and  $H_2$  permeance of  $0.2 \times 10^{-5} m^3(STP)m^{-2} s^{-1} kPa^{-1}$ , which are larger than the targets of a membrane performance suggested by Morinaga *et al.* (1992). On the other hand, the  $H_2$  and  $N_2$  permeances of S5-Z5 membrane did not show any change after 1,200-minute exposures to high temperature steam in tests I and II, resulting in a constant selectivity of 4.0.

Figures 3–5 show the Arrhenius plots of permeances before and after hydrothermal stability tests for the S9-Z1, S7-Z3 and S5-Z5 membranes, respectively. The permeation of He and  $H_2$  through the fresh S9-Z1 membrane (Fig. 3(a)) showed a characteristic of activated diffusion (permeation), in which the permeance becomes greater with the temperature in-

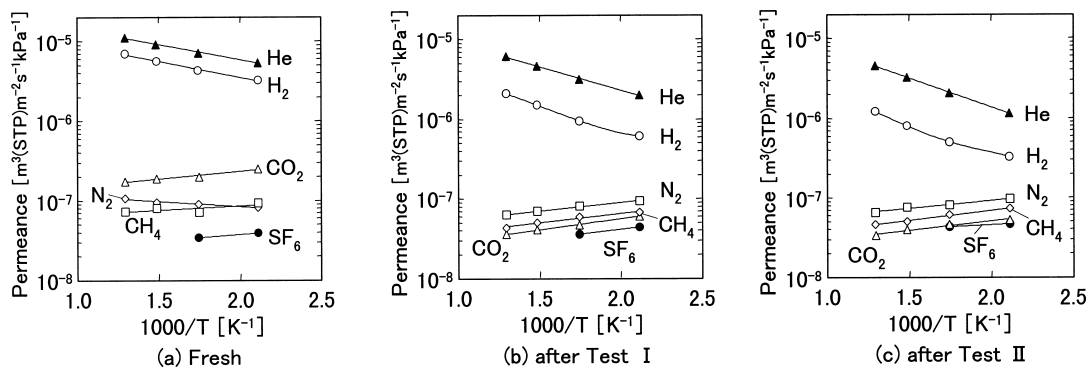


Fig. 4 Arrhenius plots of permeances through the S7-Z3 membrane before and after hydrothermal stability tests

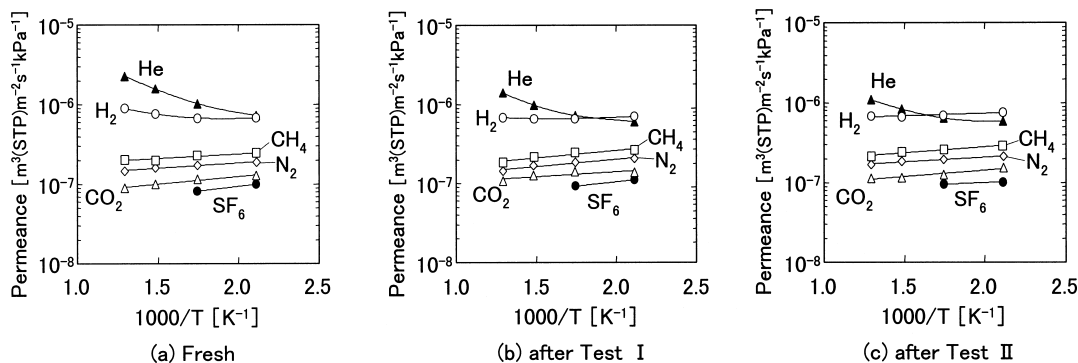


Fig. 5 Arrhenius plots of permeances through the S5-Z5 membrane before and after hydrothermal stability tests

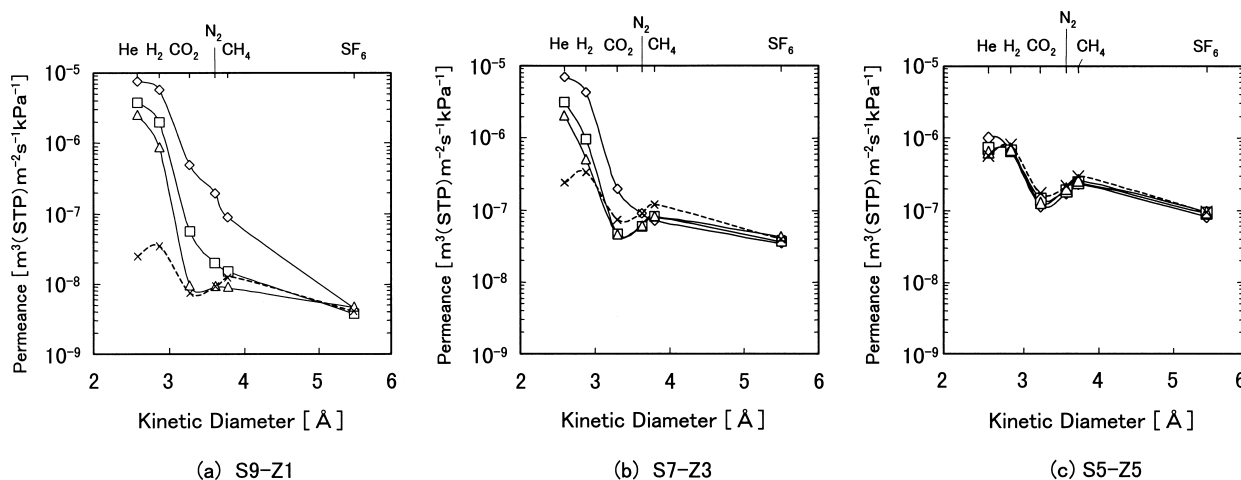


Fig. 6 Permeances for S9-Z1, S7-Z3 and S5-Z5 membranes at 300°C before and after hydrothermal stability test as a function of kinetic diameters: (◇) fresh, (□) after test I, (△) after test II and (×) Knudsen diffusion (based on SF<sub>6</sub> permeate)

crease. This tendency was strengthened after hydrothermal stability tests and the permeances of H<sub>2</sub> and He decrease as shown in Figs. 3(b) and (c). The permeation of N<sub>2</sub> and CH<sub>4</sub> through the fresh S9-Z1 membrane showed characteristics of activated diffusion, while CO<sub>2</sub> permeation seems to be due to surface diffusion. After test I, the permeances of N<sub>2</sub>, CH<sub>4</sub> and CO<sub>2</sub>

decreased drastically, and showed nearly the same value after test II. On the other hand, SF<sub>6</sub> permeance did not change before and after the hydrothermal stability tests. In case of the S7-Z3 membrane (Fig. 4), the permeances of He and H<sub>2</sub> showed a tendency similar to those of S9-Z1 membrane after the hydrothermal stability tests. Although the permeation of N<sub>2</sub>

**Table 3** Activation energy of H<sub>2</sub> and He permeation through the silica-zirconia membranes [kJ/mol]

Partial pressure of water [kPa]	H <sub>2</sub>			He		
	S9-Z1	S7-Z3	S5-Z5	S9-Z1	S7-Z3	S5-Z5
0 (fresh membrane)	3.4	8.1	44	4.7	7.6	22
40 (test I)	9.2	17.0	—	8.0	12	30
100 (test II)	13	30	—	10	15	32

through the fresh S7-Z3 membrane (Fig. 4(a)) showed the characteristic of activated diffusion, the permeation behavior changed into the Knudsen-like diffusion after test I (Fig. 4(b)), and it did not change after test II (Fig. 4(c)). The CO<sub>2</sub> permeance decreased drastically after test I, and it did not change further after test II. These results seem to show that the pores which allowed the permeation of He and H<sub>2</sub> became smaller during hydrothermal stability tests, while the pores for N<sub>2</sub>, CH<sub>4</sub> and CO<sub>2</sub> permeation changed into larger pores in which the Knudsen diffusion prevailed. The S5-Z5 membrane (Fig. 5) showed a poor selective permeation for H<sub>2</sub> and He. The He permeation showed activated diffusion, but the H<sub>2</sub> permeation showed the Knudsen-like diffusion after test I (Fig. 5(b)). For larger molecules such as N<sub>2</sub>, CH<sub>4</sub>, CO<sub>2</sub> and SF<sub>6</sub>, the permeation mechanism is the Knudsen-like diffusion. This tendency was unchanged through the hydrothermal stability tests as shown in Figs. 5(a)–(c). The results in Figs. 3–5 indicate that the H<sub>2</sub> permeance decreases with increasing ZrO<sub>2</sub> content, giving a poor ideal selectivity of  $\alpha$  (H<sub>2</sub>/N<sub>2</sub>).

**Figures 6** show the gas permeances as a function of kinetic diameters before and after hydrothermal stability tests at 300°C. The dotted curves in these figures are obtained by assuming the Knudsen diffusion based on the SF<sub>6</sub> permeance. Comparing the observed results with these dotted curves, the permeation of N<sub>2</sub>, CH<sub>4</sub> and CO<sub>2</sub> through the S9-Z1 (Fig. 6(a)) and the S7-Z3 (Fig. 6(c)) membranes shows the Knudsen-like diffusion after hydrothermal stability tests. In case of the S5-Z5 membrane (Fig. 6(c)), the permeation of N<sub>2</sub>, CH<sub>4</sub>, CO<sub>2</sub> and H<sub>2</sub> did not change even after hydrothermal stability tests, and shows the Knudsen-like diffusion. The results in Figs. 6(a) and (b) show that the pores through which N<sub>2</sub>, CO<sub>2</sub> and CH<sub>4</sub> can permeate, have vanished during hydrothermal stability tests, leaving some pinholes which seem quite stable in hydrothermal conditions.

He and H<sub>2</sub> can be considered to permeate through small pores in dense SiO<sub>2</sub>-ZrO<sub>2</sub> networks by activated diffusion. The activation energy probably depends on the ZrO<sub>2</sub> content and the tightness of the dense phase, as shown in Figs. 3–5. The activation energy can be obtained from the temperature dependency of permeance after subtracting the contribution of the Knudsen diffusion, based on N<sub>2</sub> permeance, through

**Table 4** BET surface areas of the SiO<sub>2</sub>-ZrO<sub>2</sub> powder after firing 30 minutes in air or in steamed air at 570°C [m<sup>2</sup>/g]

Firing conditions	Pure SiO <sub>2</sub>	S9-Z1	S7-Z3	S5-Z5
In air	406.7	519.7	77.4	75.0
In steam	277.9	482.4	63.3	70.4

the pinholes. **Table 3** summarizes the activation energy of H<sub>2</sub> and He permeation. The activation energies of H<sub>2</sub> and He permeation increased with increasing ZrO<sub>2</sub> content, suggesting that the network of SiO<sub>2</sub>-ZrO<sub>2</sub> matrix was densified with increasing ZrO<sub>2</sub> content. They also increased, in the hydrothermal conditions, indicating clearly that SiO<sub>2</sub>-ZrO<sub>2</sub> membranes were also densified by water vapor at high temperature.

In order to elucidate the effects of ZrO<sub>2</sub> content and water vapor at high temperature on the pores for N<sub>2</sub> permeation, specific surface areas of pure SiO<sub>2</sub>, S9-Z1, S7-Z3 and S5-Z5 powders were measured by BET method (Micromeritics, ASAP2000). These powders were prepared by drying SiO<sub>2</sub> and SiO<sub>2</sub>-ZrO<sub>2</sub> sol solutions at 150°C, and then fired in air or in steamed air (H<sub>2</sub>O: 50 kPa) at 570°C for 30 minutes. **Table 4** shows the BET surface areas of SiO<sub>2</sub> and SiO<sub>2</sub>-ZrO<sub>2</sub> powders. The specific surface area of SiO<sub>2</sub> decreased drastically, while that of S9-Z1 decreased slightly. This clearly shows that introduction of ZrO<sub>2</sub> into SiO<sub>2</sub> matrix leads to higher hydrothermal stability. But the specific surface area of S9-Z1 powder seems to decrease further by firing in higher water vapor pressure, as shown in Fig. 6(a). On the other hand, specific surface areas of S7-Z3 and S5-Z5 powders were small, suggesting that the pores for N<sub>2</sub> permeation decrease with increasing ZrO<sub>2</sub> content, as can be seen from Figs. 6(b) and (c).

## 2.2 Hydrothermal stability of membranes prepared by steam-firing

**Figure 7** compares the pure N<sub>2</sub> and H<sub>2</sub> permeances of a steam-fired membrane and an air-fired membrane at 500°C as a function of treatment time. At the beginning, H<sub>2</sub> permeances through both membranes showed almost the same value. In test I, the H<sub>2</sub> and N<sub>2</sub> permeances of an air-fired membrane decreased drastically during the first 60 minutes, and slightly from 60 to 600 minutes, as described previously. The H<sub>2</sub> and N<sub>2</sub> permeances of a steam-fired membrane did show

**Table 5** Activation energy of H<sub>2</sub> permeation through a membrane fired in steamed air and in air

Partial pressure of water vapor [kPa]	Activation energy of H <sub>2</sub> permeation [kJ/mol]	
	A membrane fired in steam	A membrane fired in air
0 (fresh membrane)	6.6	3.2
40 (test I)	7.4	9.1
100 (test II)	12.9	12.4
200 (test III)	15.2	15.5

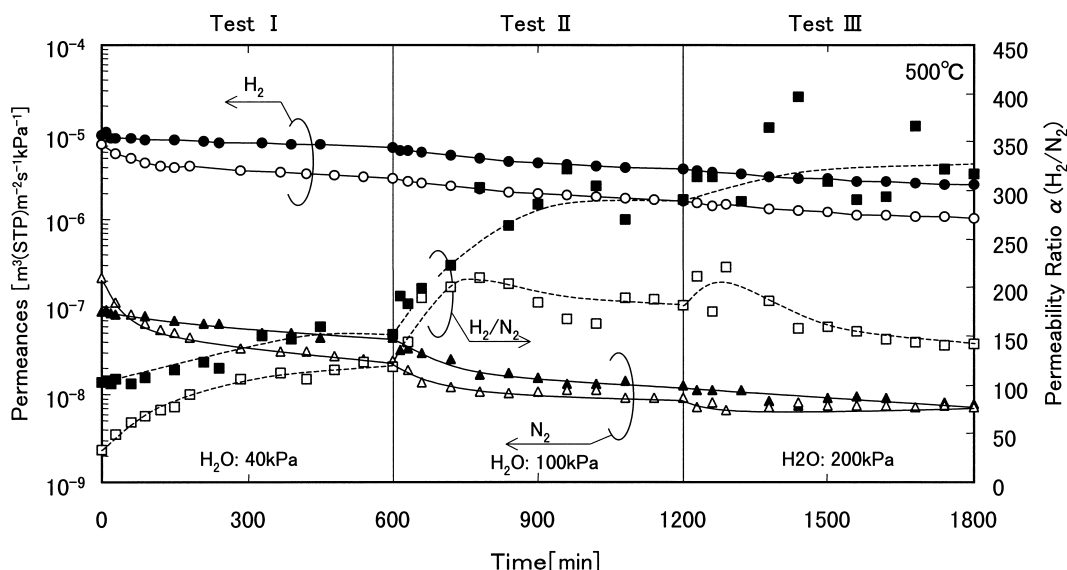


**Fig. 7** Permeances of pure N<sub>2</sub> and H<sub>2</sub> and permeability ratio  $\alpha$  (H<sub>2</sub>/N<sub>2</sub>) at 500°C as a function of hydrothermal treatment time (●, ▲, ■: a membrane fired in stream, ○, △, □: a membrane fired in air)

gradual decrease from the beginning of the test I. This is probably due to the water vapor pressure lower than that in the membrane preparation. In tests II and III, where water vapor pressure was higher than that in the membrane preparation, the H<sub>2</sub> and N<sub>2</sub> permeances through the steam-fired membrane showed the same tendency as those through the air-fired membrane. After the hydrothermal stability tests, however, the H<sub>2</sub> permeance of a steam-fired membrane showed a higher value than an air-fired membrane, while the N<sub>2</sub> permeance showed almost the same value. **Table 5** compares the activation energy of H<sub>2</sub> permeation through a steam-fired and an air-fired membrane before and after the hydrothermal stability tests. The activation energy for the steam-fired membrane increased slightly after test I and increased drastically after test II, while that of an air-fired membrane showed a step-wise increase after each hydrothermal stability test. Though a steam-firing membrane would be also densified in higher water vapor pressure at high temperature, the steam-firing methods seem to be effective to increase the hydrothermal stability of the membranes.

## Conclusion

Three types of silica-zirconia membranes with different zirconia contents were prepared by the sol-gel methods. Their hydrothermal stability and H<sub>2</sub> separation performance were tested. Some silica-zirconia membranes were also prepared by firing them in steamed air to test their stability and H<sub>2</sub> separation performance in hydrothermal conditions.

The activation energy of H<sub>2</sub> and He permeation increased with the increase in zirconia content, suggesting that the network of the silica-zirconia matrix were densified with the increase in zirconia content. The pores for N<sub>2</sub>, CO<sub>2</sub> and CH<sub>4</sub> permeation decreased with the increasing zirconia content. In the hydrothermal conditions, the activation energy of H<sub>2</sub> and He permeation also increased, indicating clearly that silica-zirconia membranes were also densified by water vapor at high temperature. In the hydrothermal conditions, the pores for N<sub>2</sub>, CO<sub>2</sub> and CH<sub>4</sub> permeation vanish, leaving some pinholes. The steam-firing method appears to be effective to increase hydrothermal stability of silica-zirconia membranes.

### Literature Cited

- Asaeda, M. and M. Kashimoto; "Sol-Gel Derived Silica Membranes for Separation of Hydrogen at High Temperature—Separation Performance and Stability against Steam—," Proc. Fifth Intern. Conf. on Inorg. Membr., p. 172–173, Nagoya, Japan (1998)
- Asaeda, M., K. Okazaki and A. Nakatani; "Preparation of Thin Porous Silica Membranes for Separation of Non-Aqueous Organic Solvent Mixtures by Pervaporation," *Ceramic Trans.*, **31**, 411–420 (1992)
- de Vos, R. M., W. F. Maier and H. Verweij; "Hydrophobic Silica Membranes for Gas Separation," *J. Membr. Sci.*, **158**, 277–288 (1999)
- Gavalas, G. R. and C. E. Megriss; "Deposition of H<sub>2</sub>-Permeable SiO<sub>2</sub> Films," *Chem. Eng. Sci.*, **44**, 1829–1835 (1989)
- Ha, H. Y., S. W. Nam and S.-A. Hong; "Fabrication and Characterization of Alumina-Silica Composite Membranes Formed by MOCVD," Proc. Fifth Intern. Conf. on Inorg. Membr., p. 62–65, Nagoya, Japan (1998)
- Hwang, G.-J., K. Onuki and S. Shimizu; "Separation of Hydrogen from a H<sub>2</sub>-H<sub>2</sub>O-HI Gaseous Mixture Using a Silica Membrane," *AIChE J.*, **1**, 92–98 (2000)
- Kikuchi, E.; "Steam Reforming and Related Reactions in Hydrogen-Permeable Membrane Reactor," *Sekiyu Gakkaishi*, **39**, 301–313 (1996)
- Kim, S. and G. R. Gavalas; "Preparation of H<sub>2</sub> Permeable Silica Membranes by Alternating Reactant Vapor Deposition," *Ind. Eng. Chem. Res.*, **34**, 168–176 (1995)
- Kitao, S., H. Kameda and M. Asaeda; "Gas Separation by Thin Porous Silica Membrane of Ultra Fine Pores at High Temperature," *Membrane*, **15**, 222–227 (1990)
- Matsumiya, N., N. Inoue, H. Mano and K. Haraya; "Effect of Water Vapor on CO<sub>2</sub> Separation Performance of Membrane Separator," *Kagaku Kogaku Ronbunshu*, **25**, 367–373 (1999)
- Mimura, T. and S. Stumi; "Evaluation of Power Loss for CO<sub>2</sub> Recovery from Flue Gas of Fossil Fuel-Fired Power Plant by Chemical Absorption Method," *Kagaku Kogaku Ronbunshu*, **24**, 546–551 (1998)
- Mimura, T., S. Stumi, T. Suda, M. Iijima and S. Mitsuoka; "Optimum Operations of CO<sub>2</sub> Recovery Process by Chemical Absorption," *Kagaku Kogaku Ronbunshu*, **24**, 1–4 (1998)
- Mimura, T., K. Matumoto, M. Iijima and S. Mitsuoka; "Applicability of Chemical Absorption Process to Carbon Dioxide Removal and Recovery under Effluent Gas Conditions of Coal-Fired Power Plant," *Kagaku Kogaku Ronbunshu*, **26**, 6–10 (2000)
- Morinaga, M., H. Moritsuka and H. Makino; "Development of CO<sub>2</sub> Recovery Thermal Power Generation Systems," Criepei Report W92029 (1992)
- Nogami, M. and Y. Moriya; "On the Properties of Non-Crystalline Films Containing TiO<sub>2</sub> and ZrO<sub>2</sub> Prepared from Metal Alkoxides—Alkali Resistance and Refractive Index—," *Yogyo-Kyokai-Shi*, **85**, 28–34 (1977)
- Sea, B.-K., K. Ando, K. Kusakabe and S. Morooka; "Separation of Hydrogen from Steam Using a SiC-Based Membrane Formed by Vapor Deposition of Triisopropylsilane," *J. Membr. Sci.*, **146**, 73–82 (1998)
- Takahashi, K., K. Watanabe and H. Moritsuka; "Hydrogen Decomposed Turbine Systems for Carbon Dioxide Recovery," Criepei Report W98011 (1999)
- Tsapatsis, M. and G. Gavalas; "Structure and Aging Characteristics of H<sub>2</sub>-Permeable SiO<sub>2</sub>-Vycor Membranes," *J. Membr. Sci.*, **87**, 281–296 (1994)
- Tsuru, T., F. Sago and M. Asaeda; "Silica and Silica-Zirconia Membranes for Hydrogen Separation at High Temperature," Proc. Fourth Intern. Conf. on Inorg. Membr., p. 111–118, Gatlinburg, TN, USA (1996)